

DOI: <https://doi.org/10.5114/pjr.2019.85147>

Received: 22.02.2019

Accepted: 10.04.2019

Published: 12.04.2019

<http://www.polradiol.com>

## Original paper

## General technical remarks on <sup>1</sup>HMRS translational research in 7T

Katarzyna Kochalska<sup>1A,B,D,E,F</sup>, Artur Łazarczyk<sup>1B,F</sup>, Anna Pankowska<sup>1B,D,F</sup>, Katarzyna Dyndor<sup>1D,E</sup>, Paulina Koziol<sup>1B,F</sup>, Andrzej Sępniewski<sup>2D,E</sup>, Radosław Pietura<sup>1D,E,F</sup><sup>1</sup>Department of Radiography, Medical University in Lublin, Poland<sup>2</sup>Centrum ECO-TECH COMPLEX Maria Curie-Skłodowska University in Lublin, Poland

### Abstract

**Purpose:** The aim of the work was to share the practical experience of preclinical and clinical proton magnetic resonance spectroscopy (<sup>1</sup>HMRS) studies conducted using a 7-Tesla magnetic field strength scanner, taking into account the specificity of both settings in the context of translational research.

**Material and methods:** <sup>1</sup>HMRS volunteer studies conducted using a Discovery 950 GE 7T scanner, were carried out with PRESS sequence, and a VOI measuring 2.0 × 2.0 × 2.0 cm<sup>3</sup> placed in the white matter at the parietal occipital lobe. Rodent spectra obtained using a 7T Bruker were measured with PRESS, with a VOI 2.0 × 2.0 × 5.5 mm<sup>3</sup> placed over the hippocampus.

**Results:** <sup>1</sup>HMRS data from humans and rats show that the brain spectra obtained in the same field are characterised by a similar neurochemical structure and spectral resolution. Spectra obtained from rats demonstrate the following metabolites: NAA, Glu, Gln, Ins, Cho, Cr, PCr, Tau, GABA, Lac, NAAG, and Asp. In turn, spectra from humans allowed estimation of the following metabolites: Ala, NAA, Glu, Gln, Ins, Cho, Cr, PCr, Tau, GABA, Lac, NAAG, and Asp. Signals from Gln, Glu with chemical shift around 2.4 ppm, from Cr, PCr, and GABA at 3 ppm, and signals from Cho and Tau at approximately 3.2 ppm, can be properly separated and estimated both in humans and in rats.

**Conclusions:** These results are promising in terms of broadening the knowledge of many neurological diseases by inducing them on animal models and then transferring this knowledge to clinical practice. In spite of this, important distinctions in the technical aspects and methodological differences of high-field <sup>1</sup>HMRS in both preclinical and clinical conditions should be taken into account.

**Key words:** <sup>1</sup>HMRS (proton magnetic resonance spectroscopy), UHF (ultra-high field), translational research.

### Introduction

*In vivo* proton magnetic resonance spectroscopy (<sup>1</sup>HMRS) is a non-invasive diagnostic modality that can measure the chemical contents from a selected region of the body. Magnetic resonance spectroscopy (MRS) allows noninvasive and quantitative assessment of metabolite levels. The MRS technique may be used in studies of a wide range of diseases across different tissues. Presently, <sup>1</sup>HMRS is most

commonly implemented in the study of the brain; generally, in diagnosing brain tumours [1], hypoxia [2], epilepsy [2], multiple sclerosis, and infection [3]. Additionally, assessment of psychiatric disorders becomes possible with the <sup>1</sup>HMRS tool, especially depression [4], panic disorders [5], and schizophrenia [5]. <sup>1</sup>HMRS is also successfully used in other anatomical areas, such as breast, liver, and prostate, allowing the estimation of tumour aggressiveness and treatment response [2,6].

### Correspondence address:

Katarzyna Kochalska, Department of Radiography, Medical University in Lublin, Poland, e-mail: [katarzynakochalska@umlub.pl](mailto:katarzynakochalska@umlub.pl)

### Authors' contribution:

A Study design · B Data collection · C Statistical analysis · D Data interpretation · E Manuscript preparation · F Literature search · G Funds collection

The strength of the main magnetic field is the key factor for the spectra quality [7]. Continuous development of superconductive magnet technology gives the opportunity to perform imaging in increasingly high strength fields [8]. The first rodent <sup>1</sup>HMRS examinations in the 7-Tesla (T) field date from the 1990s, while the feasibility of the method using a 7T scanner applied to the human brain was first demonstrated by Tkáč in 2001 [9]. Currently there are about 70 human 7T scanners installed all over the world by most leading manufacturers of MRI technology [10]. Although high field 7T systems are not allowed for use in routine clinical practice, their advantages related to increasing the main field as well as the accompanying technical developments in acquisition relevance, field shimming, pulse sequences, or parallel reception and transmission support their construction and deployment, which practically manifests itself in the growing number of clinical trials performed using 7T scanners [11].

Typically, human systems working at 7T or higher fields are referred to as ultra-high field (UHF) systems [12]. This is different from the case of preclinical systems, in which 7T has been the standard in recent decades, while many new installations are aiming towards higher fields: 9.4T, 11.7T, and 16T [13]. In the last three decades, many MRI/MRS experiments have been conducted on small animals as an introduction to clinical trials. Rodents are the most commonly used group of animals, recommended for translational studies because there are many genetically modified rodents, being animal models for a number of diseases [14,15]. Performing clinical and preclinical studies in the same field can be very useful from the point of view of possible transfer and comparison of the results [8]. Development of the technology of human high-field systems, mostly magnets, makes such studies possible and the 7T field is available both for clinical trials and preclinical, animal studies. However, practice of spectroscopy studies conducted in clinical and preclinical settings differs significantly. Patient and animal handling, available RF hardware, or problems due to field inhomogeneities may serve as examples of their specificity.

The most important advantages related to an increased main field are: increased signal-to-noise ratio (SNR) and increased spectral resolution [16]. In consequence, high-resolution spectra may be collected in a shorter time or from smaller regions, with quality high enough for precise separation of spectral lines [17,18]. However, there are also some issues related to high-field <sup>1</sup>HMRS caused by inhomogeneity of the magnetic field ( $B_0$ ) and radiofrequency field ( $B_1$ ), unwanted signals from outside the volume of interest (VOI), voxel localisation (Chemical Shift Displacement Error – CSDE), and changes in relaxation times in high-field systems [19,20].

The motivation of the work was to share the practical experience of preclinical and clinical <sup>1</sup>HMRS studies conducted at a field strength of 7T, taking into account the specificity of settings and the resulting methodological

differences in the context of translational research. The main technical issues of high-field <sup>1</sup>HMRS data acquisition in both preclinical and clinical studies are discussed.

## Material and methods

The data presented here were obtained during <sup>1</sup>HMRS volunteer studies conducted at Centrum ECO-TECH COMPLEX, equipped with a Discovery 950 GE 7T human system with maximum gradient strength of 50 mT/m and slew rate of 200 T/m/s. The configuration of the quadrature coil, with two channels for transmission and 32 channels for receiving (Nova Head 32-channel head coil, 2Tx/32Rx), was used to detect the MRS signal. <sup>1</sup>HMRS studies were carried out by SVS technique and PRESS sequence (TE/TR = 17 ms/2.500 ms, 256 averages). VOI size  $2.0 \times 2.0 \times 2.0 \text{ cm}^3$  was placed in the white matter at the parietal occipital lobe. Magnetic field homogeneity was aligned using a combination of the standard GE automated localised shimming procedure with second-order shim strategies, resulting in water line widths (full width at half maximum, FWHM) ranging from 11 Hz to 18 Hz. The signal from water was successfully suppressed by variable RF pulses with optimised relaxation delay (VAPOR).

Wistar rat studies were performed at the Centre of Experimental Medicine, Medical University in Lublin. <sup>1</sup>HMRS spectra were conducted using a 7T MRI scanner (70/16 Pharma Scan, Bruker Biospin, GmbH, Germany) using a 72 mm transceiver RF coil and a 10 mm or 20 mm receive-only surface loop coil. Maximum gradient strength and slew rate for this system is 380 mT/m and 330 T/m/s, respectively. SVS spectra were measured with PRESS sequence (TE/TR = 16 ms/2.500 ms, 1024 averages). A  $2.0 \times 2.0 \times 5.5 \text{ mm}^3$  VOI was placed over the hippocampus, avoiding contributions from tissue-tissue borders and ventricular spaces. Field homogeneity of the VOI was achieved with Localised Shim procedure, the FWHM was typically in the range of 7 to 13 Hz. VAPOR implementation was used for water suppression.

## Results and discussion

There are two main factors related to the spectrum quality, which increase significantly in high-field conditions. The first is signal-to-noise ratio (SNR), and the second is spectral resolution. Both can significantly improve the precision of identification and quantification of neurochemical profiles in animal and human studies [21,22].

The main goal of the <sup>1</sup>HMRS studies is the accurate quantification of the concentration of metabolites in selected regions of the body. The concentration is expressed in mmol/l<sup>-1</sup> or  $\mu\text{mol/g}^{-1}$  of examined tissue [2]. The strongest component of the observed signal always comes from water and is approximately 1000 times higher than the strongest metabolite signal coming from *N*-acetyl aspartate (NAA) [23]. During spectrum acquisition the water signal is

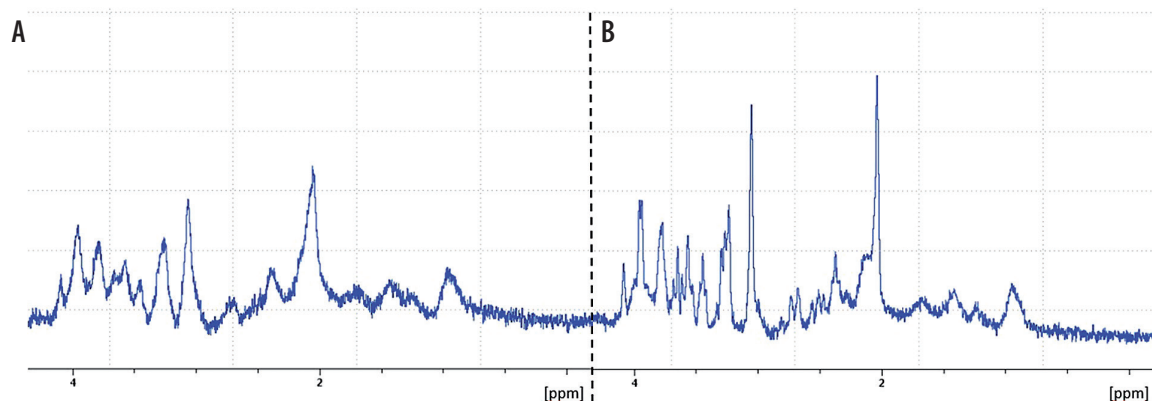


**Figure 1.**  $^1\text{H}$ MRS spectrum from rat hippocampus. Comparison of two spectra with different FWHM values. A) FWHM = 13 Hz, B) FWHM = 6 Hz. PRESS sequence: TE 16 ms, TR 2500 ms, 1024 averages, VOI size  $2 \times 2 \times 5.5 \text{ mm}^3$ . Spectral resolution determined by  $B_0$  homogeneity in the VOI (FWHM).  $B_0$  homogeneity was realised by  $B_0$  mapping technique with an additional iterative automatic shimming for higher-order shims. Spectra fitting using Top Spin software, 7 T Bruker, animal system

removed. The most popular solutions are Chemical Shift Selective Pulses (CHESS), pre-saturating water signal with the use of  $90^\circ$  frequency selective pulses followed by crusher gradients to dipphase the water signal [17] and the variable pulse power and optimized relaxation delays (VAPOR) scheme, which uses seven or eight CHESS pulses with variable flip angle and inter-pulse delays [24]. In our studies the VAPOR scheme was used. It is commonly used in MRS studies because it enables better water suppression and is less sensitive to  $T_1$  variation as well as  $B_1$  inhomogeneity [25] than CHESS, although it lasts longer and increases power deposition (SAR) [17].

On the other hand, the water signal is needed to make adjustment procedures, especially for correction of the main field homogeneity (shimming) [26]. Inhomogeneity of the main magnetic field may significantly broaden spectral lines and thus the benefits resulting from high  $B_0$  related to the increase of spectral line separation may be partially or completely lost [8]. Moreover, a broadened water line may be much more difficult to suppress without affecting metabolite lines or spectrum baseline [27]. A basic and robust shimming method is based on iterative improvement of water resonance line shape, but [28] a good experimental practice is to calculate shim currents established on acquired  $B_0$  maps, which hold information about the spatial distribution of the main field deviation in the VOI [29].

Animal  $^1\text{H}$ MRS studies, in which the VOI is generally smaller than in humans, show a lower value of water line width [25,30]. Preclinical magnets with small bore size have a more homogenous magnetic field than human systems. On the other hand, the ratio of the VOI dimension to the size of the whole brain is higher in animal studies, forcing to care about homogeneity in the VOI. A line width about 6-13 Hz was possible in animals at 7 T with the use of the  $B_0$  mapping technique with an additional iterative automatic shimming for higher-order shims, which is the standard shimming protocol offered by most vendors. Excellent  $B_0$  shimming in human studies at 7T

results in an optimal line width of about 13-18 Hz with the upper limit being the case in anatomically difficult regions, such as the frontal parts of the brain, where susceptibility effects due to the presence of air or bone are significant. Figure 1 contains spectra with different FWHM values to visualise the effect of  $B_0$  shimming on *in vivo* spectral resolution.

The water signal is also typically used for quantification, i.e. relative strengths of water lines are converted to concentrations with the use of water signal strength and some assumptions necessarily made in relation to the water content in the tissue [31]. This is the method used by software dedicated to MRS quantification, such as LCModel<sup>TM</sup> software working in the frequency domain – the most frequently selected program for spectrum analysis in clinical and preclinical settings [32]. Thus, the whole MRS acquisition must contain two spectra collected without and with water line suppression [17]. Figure 2 shows a spectrum in which the signal from water has

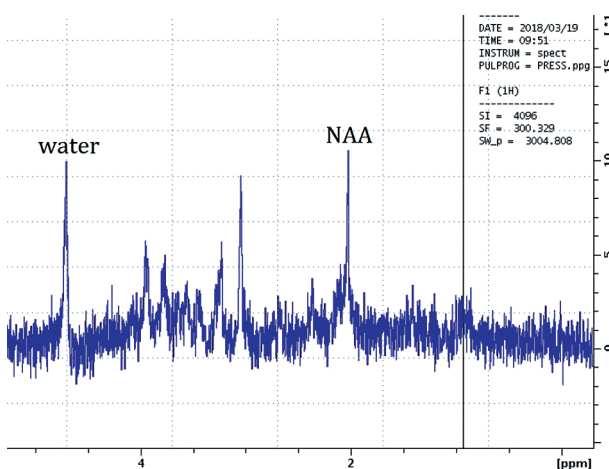


**Figure 2.**  $^1\text{H}$ MRS spectrum from rat hippocampus. PRESS sequence: TE 16 ms, TR 2500 ms, 32 averages, VOI size  $2 \times 2 \times 5.5 \text{ mm}^3$ . Attenuation of the first RF pulse in VAPOR was selected manually for each animal to reach a satisfactory level of water suppression (water signal compared to NAA). Spectra fitting using Top Spin software, 7T Bruker, animal system

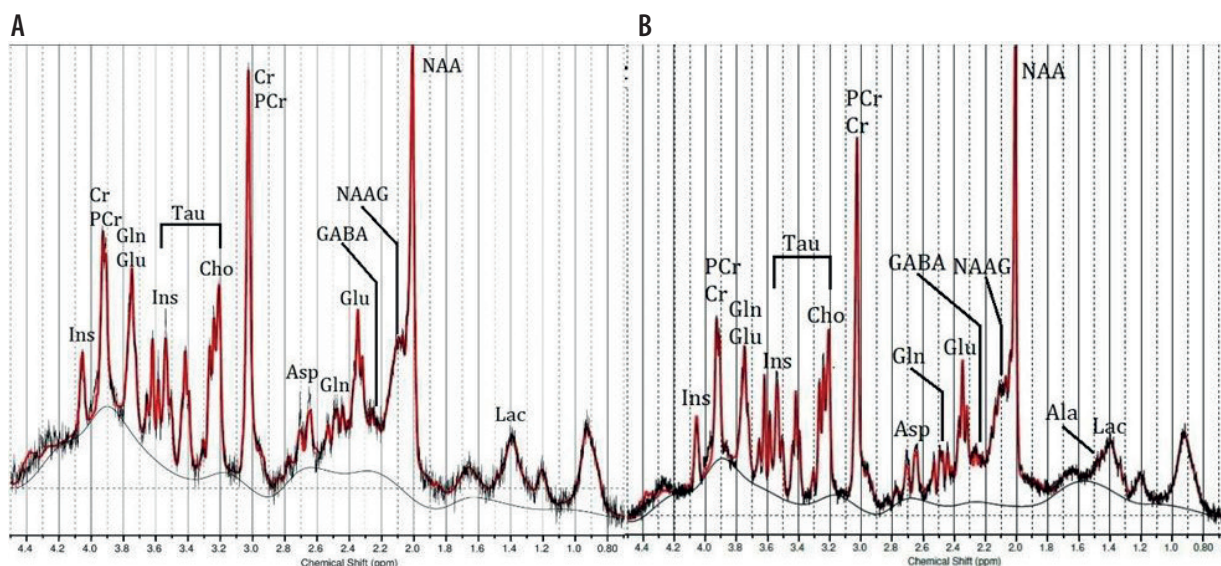


**Figure 3.** <sup>1</sup>H MRS spectra obtained at 7T. **A)** Spectrum from rat hippocampus, PRESS sequence: TE 16 ms, TR 2500 ms, VOI size  $2 \times 2 \times 5.5 \text{ mm}^3$ . **B)** Spectra from human white matter, PRESS, TE 17 ms, TR 2500 ms, VOI size  $2 \times 2 \times 2 \text{ cm}^3$ . Chemical shifts are presented relative to TMS (tetramethylsilane), ppm value on the horizontal axis in the spectra increases from right (0 ppm) to left (4.2 ppm). The window of this spectra analysis in the LCModel package was from 0.2 to 4.6 ppm. The water signal has a chemical shift value at 4.7 ppm; therefore, the water is out of range in this fitting process

comparable height to that of the NAA peak, and as a result a huge number of chemical compounds can be precisely estimated. Metabolite peaks are higher and narrower, the baseline of the spectrum is flat, and the residual water signal is present, which allows for robust estimation of the metabolite concentrations [9,32,33].

Properly adjusted <sup>1</sup>H MRS human and animal spectra in high-field systems demonstrate improved frequency separation between metabolites, as compared to lower fields [12,17], and simplifies the characterisation of multiplied signals from coupled spin systems [25]. Although increasing line separation is counteracted by the increasing width of the spectral lines due to  $T_2$  time growth, a major improvement in spectral resolution is still significant, which is related to the fact that separation between signals of coupled spins is more accurate [8]. <sup>1</sup>H MRS data from human and rat brain (Figure 3) clearly show that the brain spectra obtained in the same magnetic field are characterised by a similar neurochemical structure and spectral resolution.

Typically, spectra obtained at 7T allow the correct estimation of about 13–18 metabolites in the normal brain [34]. <sup>1</sup>H MRS spectra obtained from the rat hippocampus demonstrate the following metabolites (Figure 3): N-acetyl aspartate (NAA), glutamate (Glu), glutamine (Gln), myo-inositol (Ins), choline (Cho), creatine (Cr), phosphocreatine (PCr), taurine (Tau),  $\gamma$ -aminobutyric acid (GABA), lactate (Lac), N-acetyl aspartyl glutamate (NAAG), and aspartate (Asp). In turn, spectra from human white matter allowed the estimation of the following metabolites: alanine (Ala), NAA, Glu, Gln, Ins, Cho, Cr, PCr, Tau, GABA, Lac, NAAG, and Asp. The only difference is the missing quantification for the alanine line in the rat hippocampus spectrum. As can be seen in Figure 3, the signals from Gln, Glu with chemical shift around 2.4 ppm,

signals from Cr, PCr, and GABA at 3 ppm, and signals from Cho, Tau at approximately 3.2 ppm, can be properly separated and estimated both in humans and in rats. Also, resonance lines from NAA and NAAG were separated.

Although the background of physical processes taking place in observed tissue in animal and human studies with respect to <sup>1</sup>H MRS is assumed to be the same, there are also general differences between clinical and preclinical settings related mostly to the signal acquisition and detection or high magnetic field properties [14].

In most human <sup>1</sup>H MRS applications, there is no need to monitor physiological functions or gating appropriate for the study. A distinct procedure is applied in preclinical settings where animals are anaesthetised during the whole examination to eliminate motion artefacts, and often they are additionally immobilised in order to eliminate motion completely. Additional care is also necessary throughout the study, such as respiratory and ECG monitoring and artificial maintenance of the animal temperature in the physiological range of 36–37°C to prevent hypothermia.

In spite of an overall signal increase in high-field MRS, there is an important issue of the animal studies implied by signal loss related to a small volume of interest (VOI) [35]. The declining quality of the measured spectrum can lead to a reduction in the number of metabolites determined in the qualitative analysis. Figure 4 shows an example of a spectrum with low SNR value, in which only nine metabolites (NAA, Glu, Ins, PCho, Tau, Gln, Cr, PCr, and GABA) could be assigned, despite the preservation of the overall qualitative structure of the spectrum as compared with the corresponding spectrum with higher SNR. Increase in the SNR can be obtained by larger VOI size or additional signal averages (NA) [36]. However, attention should be paid because anaesthesia of small animals such as mice and rats should not exceed

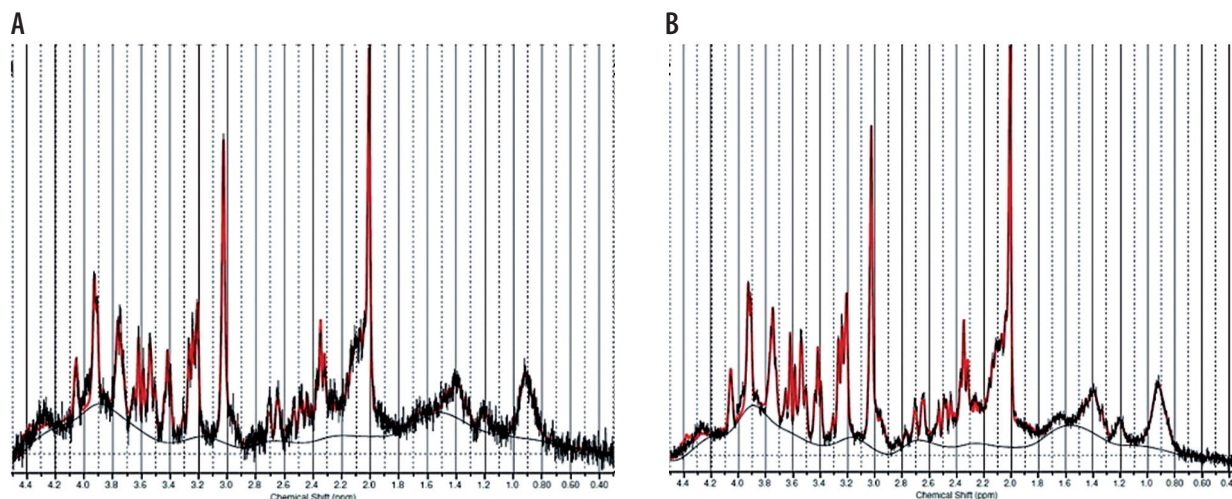


**Figure 4.** <sup>1</sup>H MRS spectrum from rat hippocampus obtained with different SNR (LCModel/ITM fit): **A)** 256 signal averages and intrinsic SNR = 22, **B)** 1024 signal averages and intrinsic SNR = 46. PRESS sequence: TE 16 ms, TR 2500 ms, VOI size 2 × 2 × 5.5 mm<sup>3</sup>. Improvement in SNR value allowed resolution of a larger number of well-fitting metabolic profiles (see discussion in the text). 7T Bruker, animal system

one hour, because changes in the level of metabolites due to the effect of the anaesthetic gases (isoflurane/oxygen mixture) are possible [37,38].

In the example of the rat brain <sup>1</sup>H MRS spectrum (Figure 4B), the above constraints mean that obtaining reasonably quantifiable data was possible for 2.0 × 2.0 × 5.5 mm<sup>3</sup> VOI size. In studies with long time of acquisition, the spectra width can increase due to B<sub>0</sub> drift. For correct compensation of the signal loss in animal studies, the number of signal averages was 1024. As a consequence, the time of acquisition was 40 minutes, and therefore the drift compensation (DC) option available with a Bruker 7 T system was used.

Usually, surface coils are used because they have higher sensitivity although for the cost of the RF field homogeneity. The latter is important for its consequences for the measurements of deeper tissue some geometrical restrictions arise instead, limiting the number of transmit and receive channels. Although four-channel receive-only phased arrays are in use, setups using single-loop receive-only coils are very common – with the diameter approximate to

the size of the examined part of the subject body, typically 10-20 mm, for small animal experiments [33].

In theory, the <sup>1</sup>H MRS spectrum comes from the signal from the selected VOI, and should not contain any contamination from the surrounding tissue [2]. However, in practice, subcutaneous lipid signals with a broad chemical shift of about 1-2 ppm can significantly deteriorate spectra quality (Figure 5). Most vendors provide a solution to this problem in the form of an OVS placed in a proper pulse sequence [39]. OVS schemes contain hyperbolic secant 90° RF pulses and crusher gradients, so unwanted coherence rephrasing can be avoided [40].

The process of selecting the VOI in high field systems has some distinct technical difficulties caused by significant spatial displacement of volumes for off-resonance signals (CSDE) from the prescribed VOI [25]. OVS applications in preclinical and clinical practice also contribute to reduction or complete elimination of CSDE [41]. Currently, the LASER method (localisation by adiabatic selective refocusing) replace the STEAM (stimulated echo

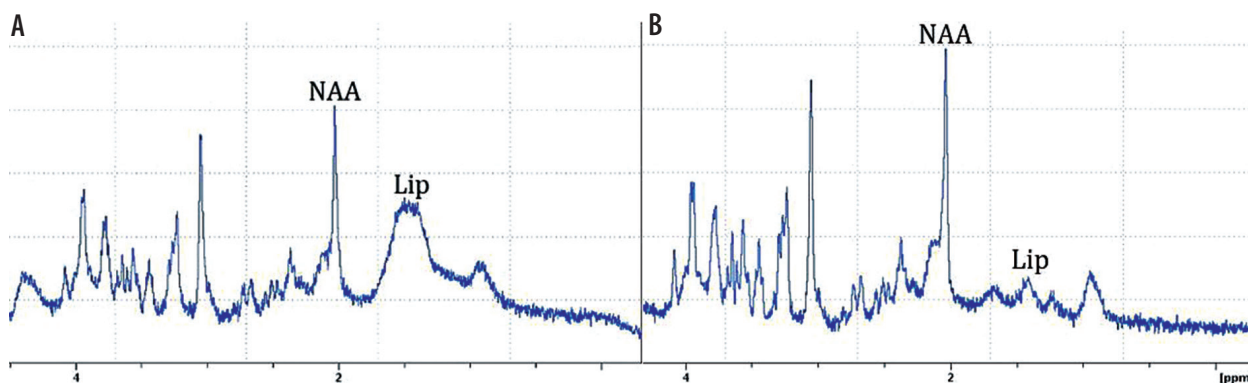


**Figure 5.** <sup>1</sup>H MRS spectrum from rat hippocampus. **A)** spectrum with big signal from lipids, **B)** spectrum with small signal from lipids. PRESS sequence: TE 16 ms, TR 2500 ms, 32 averages, VOI size 2 × 2 × 5.5 mm<sup>3</sup>. Unwanted signals from lipids can significantly disturb spectra quality. Spectra fitting using Top Spin software, 7T Bruker, animal system

acquisition mode) [39] and PRESS (point-resolved spectroscopy) [17], basic sequences offered by the vendors for high-field <sup>1</sup>HMRS studies. In LASER, the adiabatic excitation and refocusing pulses permit minimisation of the unwanted effects of the phenomenon that voxels related to different metabolites are spatially shifted due to their different resonance frequencies [42]. The subsequent increase in power deposition related to the use of long adiabatic pulses may be reduced by the use of mixed RF schemes, as has been proposed in semi-laser sequence [30]. Although localisation techniques with adiabatic pulses are not standard, they are proposed by most of MRS system vendors as available work-in-progress packages.

Human 7T RF technology faces issues of a completely different kind, related to RF field distortions originating from the fact that the length of the RF wave at 7T is comparable with the human head size [43]. In effect, multichannel transmit systems are in use which allow for an adjustment of the phase, magnitude, and pulse shape of each RF transmitter, referred to as B<sub>1</sub> shimming or RF shimming [44]. B<sub>1</sub> shimming is not yet widespread in UHF human research practice due to the fact that multiple excitation coils and specialised RF hardware are required [8]. B<sub>1</sub> non-uniformity causes fluctuations of the signal intensity and decreases the SNR of the MRS data [33]. As a consequence, B<sub>1</sub> non-uniformity, may disturb the direct interpretation of MRS spectra. <sup>1</sup>HMRS animal examinations have fewer technical problems due to generating insufficient strength of B<sub>1</sub> because of the small size of the RF coils [33].

When moving the <sup>1</sup>HMRS experiment from preclinical to clinical settings at 7T, the consideration about SAR restriction should always be taken into account. SAR is the quantity of energy deposited in imaged tissues by RF pulses, and it is proportional to the square of the electric field strength [43]. The magnitude of the electric field depends both on the B<sub>1</sub> amplitude and its change rate, hence it grows considerably with B<sub>0</sub> strength. The United States Food and Drug Administration (FDA) and the International Electrotechnical Commission have established SAR limits for the human body [42]. According to these guidelines, the SAR value for the head should not exceed 4 W/kg, 8 W/kg for the torso, and 12 W/kg for the extremities [43]. However, it should be remembered that highly heterogeneous B<sub>1</sub> may produce SAR locally exceeding globally accepted values [45]. A slightly different situation is encountered in preclinical imaging. In rodents the blood exchange is faster

due to their considerably smaller size. Moreover, the animal body temperature is maintained artificially and controlled during scanning. Typically, the animal imaging system has no rigid restrictions for SAR limits [14].

Interestingly, despite the fact that the <sup>1</sup>HMRS method has been developed for many years, there are still no guidelines regarding the analysis of the results, i.e. the adjustment of spectra. There is basically no standard methods of data processing and quantification, and they still differ between clinical or preclinical laboratories [41]. Spectra quantification is generally not straightforward due to the occurrence of different assessment approaches [46]. It is possible that in the future, thanks to the further development of <sup>1</sup>HMRS technology and new solutions for the principles of coherent quantification for all scientists, this method will find even greater application in clinical practice [47].

## Conclusions

<sup>1</sup>HMRS *in vivo* techniques combined with high magnetic field are capable of providing information on a large range of neurometabolites with high accuracy. These results are promising in terms of broadening the knowledge about many neurological diseases by inducing them on animal models and then transferring this knowledge to clinical practice. Continuous development of magnetic resonance technology gives an opportunity for transferability of experiences from preclinical to clinical settings and for translational research in the same field. In spite of this, the important distinction in the technical aspects and methodological differences of high-field <sup>1</sup>HMRS in both preclinical and clinical conditions should be taken into account.

## Acknowledgments

The authors would like to thank Dr. Tomasz Skórka from the Department of Magnetic Resonance Imaging, Institute of Nuclear Physics, Polish Academy of Sciences in Krakow for analysis of the <sup>1</sup>HMRS spectra in the LCModel software and for comments to the manuscript. This research was funded by the Medical University in Lublin, as part of the research project with the number MNmb 578.

## Conflict of interest

The authors report no conflict of interest.

## References

1. Polimeni JR, Uludağ K. Neuroimaging with ultra-high field MRI: Present and future. *Neuroimage* 2018; 168: 1-6.
2. Barker P. *Clinical MR spectroscopy: Techniques and applications*. Cambridge University Press, Cambridge 2010.
3. Prinsen H, Graaf RA de, Mason GF, et al. Reproducibility measurement of glutathione, GABA, and glutamate: Towards *in vivo* neurochemical profiling of multiple sclerosis with MR spectroscopy at 7T. *J Magn Reson Imaging* 2017; 45: 187-198.

4. Lee TS, Quek SY, Krishnan KRR. Molecular imaging for depressive disorders. *AJNR Am J Neuroradiol* 2014; 35: S44-S54.
5. Godlewska BR, Clare S, Cowen PJ, Emir UE. Ultra-High-Field Magnetic Resonance Spectroscopy in Psychiatry. *Front Psychiatry* 2017; 8: 123.
6. Faghilhi R, Zeinali-Rafsanjani B, Mosleh-Shirazi MA, et al. Magnetic Resonance Spectroscopy and its Clinical Applications: A Review. *Journal of Medical Imaging and Radiation Sciences* 2017; 48: 233-253.
7. Terpstra M, Cheong I, Lyu T, et al. Test-retest reproducibility of neurochemical profiles with short-echo, single-voxel MR spectroscopy at 3T and 7T. *Magn Reson Med* 2016; 76: 1083-1091.
8. Hennig J, Speck O. *High-Field MR Imaging*. Springer, Berlin Heidelberg, 2012.
9. Tkáč I, Andersen P, Adriany G, et al. In vivo 1H NMR spectroscopy of the human brain at 7 T. *Magn Reson Med* 2001; 46: 451-466.
10. Donatelli G, Ceravolo R, Frosini D et al. Present and Future of Ultra-High Field MRI in Neurodegenerative Disorders. *Curr Neurol Neurosci Rep* 2018; 18: 31.
11. Nakada T. Clinical application of high and ultra high-field MRI. *Brain Dev* 2007; 29: 325-335.
12. Henning A. Proton and multinuclear magnetic resonance spectroscopy in the human brain at ultra-high field strength: A review. *Neuroimage* 2018; 168: 181-198.
13. Uğurbil K. Imaging at ultrahigh magnetic fields: History, challenges, and solutions. *Neuroimage* 2018; 168: 7-32.
14. Schröder L. *In vivo NMR Imaging Methods and Protocols*. Humana Press 2011; 12-20.
15. Hermann D, Weber-Fahr W, Sartorius A, et al. Translational magnetic resonance spectroscopy reveals excessive central glutamate levels during alcohol withdrawal in humans and rats. *Biol Psychiatry* 2012; 71: 1015-1021.
16. Ladd ME, Bachert P, Meyerspeer M, et al. Pros and cons of ultra-high-field MRI/MRS for human application. *Prog Nucl Magn Reson Spectrosc* 2018; 109: 1-50.
17. Bottomley PA, Griffiths JR (ed.). *Handbook of magnetic resonance spectroscopy in vivo: MRS theory, practice and applications*. Chichester, Wiley, 2016.
18. McKay J, Tkáč I. Quantitative in vivo neurochemical profiling in humans: where are we now? *Int J Epidemiol* 2016; 45: 1339-1350.
19. Tkáč I, Gruetter R. Methodology of H NMR Spectroscopy of the Human Brain at Very High Magnetic Fields. *Appl Magn Reson* 2005; 29: 139-157.
20. Lopez-Kolkovsky AL, Mériaux S, Boumezbear F. Metabolite and macromolecule T1 and T2 relaxation times in the rat brain in vivo at 17.2T. *Magn Reson Med* 2016; 75: 503-514.
21. Buonocore MH, Maddock RJ. Magnetic resonance spectroscopy of the brain: a review of physical principles and technical methods. *Rev Neurosci* 2015; 26: 609-632.
22. Cao Z, Park J, Cho Z-H, Collins CM. Numerical evaluation of image homogeneity, signal-to-noise ratio, and specific absorption rate for human brain imaging at 1.5, 3, 7, 10.5, and 14T in an 8-channel transmit/receive array. *J Magn Reson Imaging* 2015; 41: 1432-1439.
23. Kreis R, Ernst T, Ross BD. Absolute Quantitation of Water and Metabolites in the Human Brain. II. Metabolite Concentrations. *J Magn Reson B* 1993; 102: 9-19.
24. Tkáč I, Andersen P, Adriany G, et al. In vivo 1H NMR spectroscopy of the human brain at 7 T. *Magn Reson Med* 2001; 46: 451-466.
25. de Graaf RA. *In vivo NMR spectroscopy: Principles and techniques*, 2<sup>nd</sup> ed. John Wiley & Sons, Chichester, West Sussex, England, Hoboken, NJ, 2007.
26. Juchem C, de Graaf RA. B0 magnetic field homogeneity and shimming for in vivo magnetic resonance spectroscopy. *Anal Biochem* 2017; 529: 17-29.
27. Cabanes E, Confort-Gouny S, Le Fur Y, et al. Optimization of residual water signal removal by HLSVD on simulated short echo time proton MR spectra of the human brain. *J Magn Reson* 2001; 150: 116-125.
28. Chang P, Nassirpour S, Henning A. Modeling real shim fields for very high degree (and order) B0 shimming of the human brain at 9.4 T. *Magn Reson Med* 2018; 79: 529-540.
29. Nassirpour S, Chang P, Fillmer A, Henning A. A comparison of optimization algorithms for localized in vivo B0 shimming. *Magn Reson Med* 2018; 79: 1145-1156.
30. Giapitzakis IA, Shao T, Avdievich N, et al. Metabolite-cycled STEAM and semi-LASER localization for MR spectroscopy of the human brain at 9.4T. *Magn Reson Med* 2018; 79: 1841-1850.
31. Ernst T. Absolute Quantitation of Water and Metabolites in the Human Brain. I. Compartments and Water. *J Magn Res B* 1993; 102: 1-8.
32. Provencher SW. Automatic quantitation of localized in vivo 1H spectra with LCModel. *NMR Biomed* 2001; 14: 260-264.
33. Xin L, Tkáč I. A practical guide to in vivo proton magnetic resonance spectroscopy at high magnetic fields. *Anal Biochem* 2017; 529: 30-39.
34. Pfeuffer J, Tkáč I, Provencher SW, Gruetter R. Toward an in vivo neurochemical profile: quantification of 18 metabolites in short-echo-time (1)H NMR spectra of the rat brain. *J Magn Reson* 1999; 141: 104-120.
35. Fleysher R, Fleysher L, Liu S, Gonen O. On the Voxel Size and Magnetic Field Strength Dependence of Spectral Resolution in MR Spectroscopy. *Magn Reson Imaging* 2008; 27: 222-232.
36. Kirchner T, Fillmer A, Henning A. Mechanisms of SNR and line shape improvement by B0 correction in overdiscrete MRSI reconstruction. *Magn Reson Med* 2017; 77: 44-56.
37. Söbbeler FJ, Carrera I, Pasloske K, et al. Effects of isoflurane, sevoflurane, propofol and alfaxalone on brain metabolism in dogs assessed by proton magnetic resonance spectroscopy (1H MRS). *BMC Vet Res* 2018; 14: 69.
38. Makaryus R, Lee H, Yu M, et al. The metabolomic profile during isoflurane anesthesia differs from propofol anesthesia in the live rodent brain. *J Cereb Blood Flow Metab* 2011; 31: 1432-1442.
39. Skoch A, Jiru F, Bunke J. Spectroscopic imaging: basic principles. *Eur J Radiol* 2008; 67: 230-239.
40. Tkáč I, Gruetter R. Methodology of H NMR Spectroscopy of the Human Brain at Very High Magnetic Fields. *Appl Magn Reson* 2005; 29: 139-157.
41. Kreis R. Issues of spectral quality in clinical 1H-magnetic resonance spectroscopy and a gallery of artifacts. *NMR Biomed* 2004; 17: 361-381.
42. Scheenen T, Klomp D, et al. Short echo time 1H-MRSI of the human brain at 3T with minimal chemical shift displacement errors using adiabatic refocusing pulses. *Magn Reson Med* 2008; 59: 1-6.

43. Collins CM, Smith MB. Calculations of B(1) distribution, SNR, and SAR for a surface coil adjacent to an anatomically-accurate human body model. *Magn Reson Med* 2001; 45: 692-699.
44. Shao Y, Shang S, Wang S. On the safety margin of using simplified human head models for local SAR simulations of B1-shimming at 7 Tesla. *Magn Reson Imaging* 2015; 33: 779-786.
45. Collins CM, Liu W, Wang J, et al. Temperature and SAR calculations for a human head within volume and surface coils at 64 and 300 MHz. *J Magn Reson Imaging* 2004; 19: 650-656.
46. Helms G. The principles of quantification applied to in vivo proton MR spectroscopy. *Eur J Radiol* 2008; 67: 218-229.
47. Stagg C, Rothman DL. *Magnetic Resonance Spectroscopy: Tools for Neuroscience Research and Emerging Clinical Applications*. Elsevier Science, Burlington, 2014.